



A New Extracted Features to Recognize Faces Effected by Occlusions and Common Variations

Ahmad Bany Doumi¹, Feras E. Abualadas², Mohammed M. Abu Shquier^{1,*}, Mahmoud Asassfeh³, Bassam Mohammad Elzaghmouri¹, Khaled M. Alhawity⁴

¹ Faculty of Computer Science and Information Technology, Jerash University, Jerash, Jordan

² Department of Cyber Security-Faculty of Computer Science and Informatics, Amman Arab University, Amman, Jordan

³ Department of Cyber Security- Faculty of Information Technology, Zarqa University, Zarqa, Jordan

⁴ Faculty of Computes and IT, University of Tabuk, Tabuk, Saudia Arabia

ABSTRACT

Face recognition from non-identical face photos is a prominent area of research in pattern recognition and computer vision. Existing face recognition systems struggle with diverse changes like lighting conditions, expressions, and facial occlusions. This paper proposes a new Face Recognition (FR) approach that combines the Elastic Bunch Graph Matching (EBGM) approach with the greedy algorithm to automatically identify face landmarks. The proposed approach independently selects each optimal landmark of face image from different corresponding face images where the corresponding landmark of corresponding face image which achieves the best similarity is used rather than using one or at most two corresponding face images and computing the average between both. The locations of corresponding landmarks can be displaced to achieve maximum similarity with optimal landmarks. This proposed approach demonstrates improved recognition performance compared to contemporary face recognition methods. It effectively handles changing ratios of face parts and can recognize faces even with increasing occlusion sizes.

Keywords:

EBGM; Greedy algorithm; Face graph;
Jet

1. Introduction

Face recognition has gained significant attention among researchers in various fields, including banking and criminalistics [1]. With the advancement of computer applications that can process images and video frames, the interest in face recognition systems has grown [2-4]. Researchers are now focusing on developing efficient face recognition systems that can identify faces despite occlusions or other differences. This is particularly important in real-life scenarios where thieves and criminals often use scarves or sunglasses to conceal their identities. Face recognition applications compare face images stored in a database with a given face to find the closest match [5]. However, challenges such as facial occlusions, expressions, and lighting variations have affected the

* Corresponding author.

E-mail address: shquier@jpu.edu.jo

effectiveness of these applications [5,6]. To address these challenges, different approaches have been suggested [7-9]. One approach is the holistic approach, which treats the entire face as a single component. It uses global information from facial images to distinguish between faces [10-13]. Another approach is the component-based system, which divides the face into segments for independent analysis. This allows for flexibility in accounting for changes in face. In the component-based face identification approach, the components show less variance under pose changes than the entire face image pattern [14,15].

After detecting occluded parts of the facial picture, the methodologies can deal with the occluded blocks by reconstructing them, discarding them, or treating them as other areas [16]. Elastic Bunch Graph Matching (EBGM) is a holistic face recognition technique that considers local features such as eyes and nose, and their geometric relationships [17,18]. EBGM is based on the construction of a face image graph to describe a high-dimensional facial picture in a lower dimension [1]. The fundamental idea behind EBGM is to identify a particular number of landmarks in a facial image [19-21]. It is worth noting that EBGM may tolerate some degree of pose and expression alterations and still produce successful results [22]. The Gabor wavelets transform is then calculated for each selected landmark in order to discover the same place in other face images by attaining the most similarities with the landmarks in other face images. A jet is the process of localizing landmarks using Gabor wavelets transformations. Face Bunch Graph (FBG) is a group of jets from the same landmark area in different photos. Thus, the landmark points of a fresh facial image are chosen by matching them with the FBG that has the highest resemblance. The average distance between previously located landmark points in FBG is used to predict the beginning position of new landmark points [20].

Metaheuristic algorithms (greedy algorithm) were used to automatically determine landmark points without human intervention to achieve higher recognition rates [23-28]. This approach describes a method for recognizing faces obscured by occlusions and other modifications. The EBGM technique is used when the optimal landmarks are found by a metaheuristic algorithm [23]. Then, the similarity for each optimal landmark is used. The proposed approach will be applied and evaluated on the AR dataset and the modified AR dataset [29].

2. Background

In this section, an overview of Elastic Bunch Graph Matching (EBGM) is introduced. Also, the metaheuristic algorithm wherein the greedy algorithm that have been used in the proposed approach are presented.

2.1 Elastic Bunch Graph Matching (EBGM)

Elastic Bunch Graph Matching (EBGM) algorithm was initially proposed in [22] where it was used by the Colorado State University (CSU) as a baseline approach for comparing facial recognition systems and it is one of the most widely used facial recognition algorithms [20].

The EBGM technique steps are illustrated in [5,30]. To recognize a face (probe face image) by comparing it with reference face images stored in the database, at first many landmark points have to be defined to represent the probe face image [5]. For example, the set of all located landmarks in face images is represented by Landmark Points (LP) matrix as shown in Eq. (1).

$$LP = \begin{pmatrix} (x_1, y_1) & \dots & (x_2, y_2) \\ & \dots & (x_3, y_3) & \dots \\ (x_4, y_4) & \dots & (x_5, y_5) \end{pmatrix} \quad (1)$$

Where LP matrix nodes are the corresponding landmarks inside one of the face images where each node such as (x_1, y_1) is a point for the first landmark of face images Where the Gabor wavelet transform will be calculated for each node (landmark point) in the LP matrix with orientations (O_r) defined as $\mu = (0, 1, \dots, O_r - 1)$ and frequencies (F_r) defined as $v = (0, \dots, F_r - 1)$. In the literature, the values of O_r equals 8 and F_r equals 5, are suggested in [5,20,31,32]. Thereafter, a total of $O_r \times F_r$ complex coefficients is created for each landmark point. The vector Jet (J) of the length $O_r \times F_r$ coefficients is computed for each landmark in the LP matrix by convolving with a different of wavelets. In general, the Jet (J) is a small patch of grey values for a particular image $I(\vec{x})$ around a specific input pixel [5] where \vec{x} and \vec{x}' is all landmark points stored in the LP matrix.

As previously stated, the length of a Jet vector (J) has $O_r \times F_r$ complex coefficients $J = (a_1, a_2, \dots, a_{O_r \times F_r})$ where the total of $O_r \times F_r$ magnitude values ($|a_1|, |a_2|, \dots, |a_{O_r \times F_r}|$) and a total of $O_r \times F_r$ phase θ ($\theta_1, \theta_2, \dots, \theta_{O_r \times F_r}$) represent the J vector.

The similarity between the landmark points and corresponding landmark points in two different images are computed using their Jet vectors. To determine the landmark points automatically as in [5] the model and reference images will be utilized to locate the optimal landmark points where model images contain image variations such as occlusion (scarf and sunglasses), illumination, and expression. Usually, the model images have the most similar variations with probe images which must be recognized by the landmarks determined by that model image. The reference image, on the other hand, is a neutral image stored in the face database and is used to match a given probe image.

Transformation is one of image processing techniques which it is used to construct masks where these masks will be convoluted with jet vectors. Examples of transform techniques are Wavelet, Fourier, Hilbert, Radon transforms which they are used to analyse frequency space properties of an image [33]. The two most popular types are Gabor wavelets and Fourier transforms where the Gabor wavelets are considered as fundamental to the EBGGM technique. The difference between the two is that wavelets operate on a localized image patch, while the Fourier transform operates over the entire image [20]. The wavelet transform is a technique which assimilates the time and frequency domains and precisely popular as time-frequency representation of a non-stationary signal [33].

To represent the similarity equations mathematically, suppose that J and J' are the jet vectors created from the landmarks of model and reference images, respectively. The goal is to identify the optimal landmarks in the face images that increase the similarity of the corresponding J and J'. As a result, the objective function is determined as follows:

$$f(x) = \max S(J, J') \tag{2}$$

$$S(J, J') = \frac{\sum_j |a_j| |a'_j| \cos(\theta_j - \theta'_j)}{\sqrt{\sum_j |a_j|^2 \sum_j |a'_j|^2}} \quad \forall j \in J, J' \tag{3}$$

2.2 Greedy Algorithm

Greedy is an algorithm that assembles a solution piece by piece, always selecting the next component that provides the greatest evident and immediate benefit. So Greedy is best suited to cases when choosing locally optimal also leads to a global solution.

The fundamental purpose of this technique is that the decision is made based on the information that is now accessible. Whatever current information is available, the decision is taken without regard for the long-term consequences of the current decision.

This technique is used to find the most feasible solution, which may or may not be optimal [34]. A practicable solution is a subset that meets the specified requirements. The best and most beneficial solution in the subset is called the optimal solution. In the case of feasible, if more than one solution meets the required requirements, those alternatives are deemed viable, whereas the optimal solution is the best answer among all possible solutions [35]. Algorithm 1 shows the steps of Greedy algorithm.

Algorithm 1 Greedy Algorithm

Input: Problem space

Output: The best solution for that problem

```
1 Solution ← 0 //The solution is given a value of zero.
2 for i = 0 to z do
3   x = select(c); //Choose the elements one by one
4   if feasible(solution, y) then //Determines whether or not the solution is
   feasible
5     Solution: = union (solution, y) //Carry out the union and return the result if
6     return solution; // the solution is feasible
7   end if
8 end for
```

3. Related Work

A number of strategies for face recognition have been proposed in the past few years. These methods can achieve high performances on good quality data which are captured in controlled conditions. Generally, some of these researches are summarized below with different techniques related to face recognition under occlusion and several variations.

3.1 Face Recognition Approaches

Gao and Leung [36] Proposed the Line Edge Map technique where the face contours are obtained and collected in segments, and then organized in lines. To manipulate these new feature vectors, the Hausdorff distance has been customized to manage them. Also, they discussed a new pre-filtering criterion for screening the whole collection of individuals to conduct the real testing operation. This technique has been tested on different conditions as illumination and expression. The results showed that it outperforms other techniques such as Eigen-faces presented in [37]. This approach didn't investigate the occlusion cases.

Kanan *et al.*, [38] presented an Adaptively Weighted Patch Pseudo Zernike Moment Array (AWPPZMA) as a features extraction technique to extract features from local patch after divide the image of face to small local patches. AWPPZMA matching score used for recognition process for the probe face image. Where AWPPZMA evaluated by different facial expressions, illumination conditions and partial occlusion. The results show that AWPPZMA. It more efficiency than other techniques such as Modular PCA presented in [39]. In this approach, the occlusion cases were not investigated.

A face recognition system was presented by Kanan and Faez [16] based on a component-based model based on Adaptively Weighted Sub-Gabor Array (AWSGA). This technique was introduced when there is one sample for face image per available enrolled subject. Faces divided in to sub-patterns based on AWSGA a local Gabor array in addition, n Augmented SG Array (ASGA) of the face

image constructs using a Sub-Gabor Wavelet (SGW) operation. AWSGA considered the occlusions as local distortions faraway from face that represents the human individuals. Where comparison between each local area that represent as input face image with the corresponding local area in the general face image of human can be used to measurement these distortions. This measurement used by AWSGA to weight individual Sub-Gabor elements of each region. The experimental results show a good result with lower face occlusions and bad result (recognition rate) with upper face occlusions when using this approach.

Chen and Gao [40] proposed a technique that represents face based on string and process it to find the low-level features letters. These features grouped into intermediate-level words after that collected words are integrated into high-level sentence strings using their relational organization. Matching done between two images, string -to-string. Where this technique defines the most significant local parts (substrings) for recognition. Also, this way of similarity helps in problem of occlusion. However, this technique is affected by the accuracy of line segmentation.

Venkat *et al.*, [8] introduced an approach for recognize occluded faces based on Psychophysically Inspired Similarity Mapping (PISIMA) instead of holistic approach to processes the local facial components. The local features extracted using Bayesian network model. Where these features included in horizontal sub-regions of image based on evidence obtained from the psychological domain. This technique, however, needs many face images for training.

Lahasan *et al.*, [5] introduced HSO-EBGM based on the EBGM and Harmony Search Oriented (HSO) algorithms for face recognition under occlusion and some of common difference, such as illumination and expression. Where image of face was dividing into six segments, separately each one recognized. In addition, exploited the HSO algorithms to maximize similarity based on determine the optimal facial landmarks automatically. Where HSO-EBGM grant face recognitions applications a property to be automatic completely without depend on manual ground truth data to find face recognition landmarks. Distinguished between one face and another was computed through the averaging the similarity exist on their corresponding component-level partial face-graphs. In this approach the recognition of occluded faces without needed for any knowledge or assumption in advance about occluded regions. Where any occluded region does not ignore from calculations nor reconstructs this region, HSO-EBGM manipulate with-it partial occlusions same as other regions. To measure the performance in terms of recognition rate HSO-EBGM was used with (AR and FRGC ver. 2.0) databases. However, this method is depending on average similarity which leads to minimize the accuracy by increasing the number of landmarks located in the occlusion block.

Alsalibi *et al.*, [9] presented a facial feature selection depends on a new membrane-inspired binary bat technique. Where high-dimensional local binary pattern and Gabor wavelet were obtained from face and combined as features, based on a binary bat algorithm using canonical correlation analysis. The experimental results show that this technique make better than other face recognition techniques on three benchmark databases such as sparse representation-based classification presented in [41]. In other hand show bad results against upper faces occlusion.

Angadi and Hatture [17] focused in face recognition with lighting and partial occlusion based on symbolic data analysis and a multiclass support vector machine. Where three set of connected graphs define the face image, each set represented by a symbolic entity. Graph spectral properties and energy was derived and combined into symbolic object. To asses results two database was used. The experimental results show that the recognition rate achieved 95.97% with AR face database and 97.20% with VTU-BEC-DB multimodal.

Varma *et al.*, [42] proposed an algorithm for facial recognition based on a histogram, where the region of face was divided into several regions. The values of histogram extracted are connect with single vector. Where the best results given by compared the vector with similarities between the

facial images. In this algorithm the case of occlusion was not investigated. In other hand, how often the gradient orientation appears in localized portions of an image was calculated.

Cheng and Pan [43] proposed two methods to solve the problem of occlusion in modern face recognition: occlusion region restore and occlusion location based on attention. Where they studied the mainstream general ways classifiers of linear regression to dealing with occlusion problems, such as dictionary representation of occlusion, learning and compression techniques of occlusion dictionaries and collaborative representation. This research showed the important of feature extraction technique in occluded face recognition solving, and highlighted to some of important problem and challenges such as: using convolution neural networks, optimization algorithms and feature extraction.

Ma *et al.*, [44] introduced a method to solve the occlusion problem of the real-world face recognition by construct a constrained probabilistic sparse representation network to obtain the images features that the training from global perspective. Where the new node generated for network are constructed from random combination of training images. Each class probability was calculated and defines individually for image belongs to sparse subspace. Where the maximum common probability of the network nodes used to determine the final test image classification. The experimental results show that the second-order gradient constraint in the probabilistic sparse representation network, which can better distinguish between the occlusion and non-occlusion parts.

Hemathilaka and Aponso [45] has presented a comprehensive analysis for strategies of occluded face recognition included face mask occlusion based on detail comparisons, also they classified approaches based on systematically way, into occlusion (robust, discard and recovery). In addition, they discussed how approaches of deep learning and occlusion of face mask effect the face recognition. Finally, they address some of challenges of face recognition and their solution that can help in improvement the face recognition domain based on face mask occlusions, where discussion shows that false rejection rate between 20% and 50% in most algorithms if the percentage of mask around 70% of face, in addition, the quite competitive algorithm the give, Minimum failure rate (5%) when mask is less than 70%.

Moungsouy *et al.*, [46] developed a solution to improve the performance of face recognition in both without mask-wearing and mask-wearing based on the FaceNet framework using residual inception network of Inception-ResNet-v1 architecture, using any facial components is available. Where simulated masked-face images are computed from the top of face and used for learning process. Also, heatmaps features are used and drawn that is important for face recognition. The experimental results shows that the accuracy is 99.2 in mask-wearing faces in addition, non-occluded components including nose and eyes become more important for human face recognition in comparison with lower part of human face which can be occluded under masks.

Chen *et al.*, [47] proposed a feature fusion residual attention network (FFRA-Net) to process expression features loss. Where by using FFRA-Net the intermediate feature map divides into different sub-feature maps in an equal manner along the channel dimension using a multi-scale module to obtain diverse global features by applied convolution operation to each feature map. In addition, FFRA-Net divide the intermediate features in to different sub-features maps along the spatial dimension using local attention module to extraction a local key features through the attention mechanism. Where the concatenation between local expression and global features. It is done through feature fusion module in addition to create residual links between (inputs and outputs) to compensate for the loss of fine-grained features. The experimental results show that the proposed model achieved an excellent result with FM_RAF-DB, SG_RAF-DB, RAF-DB, and FERPLUS with

accuracies of 77.87%, 79.50%, 88.66%, and 88.97%, respectively. This model is very effective in occluded facial expression recognition.

3.2 Summary of Related Work

By studying the related work of face recognition to explore more about recognizing the occluded faces and faces under real variations by EBGM and other techniques. Accordingly, the weak points of the EBGM technique, which is reducing the recognition rates, especially in the presence of the occlusion, have been investigated.

In the proposed approach, the technique used for the recognition is hybridized where the EBGM and greedy algorithms is integrated to locate the landmark points of EBGM. Each landmark connects with other landmarks of the image. Further, the proposed technique relies on EBGM equations.

The novel approach aims to reduce the impact of investigated problems and enhance the recognition rate. In the proposed approach, the similarity between the jet of optimal landmark point of an image and the jet of corresponding landmark point of another image is computed for two images at the same time and the corresponding landmark point is located in the same landmark position or in nearest-neighbour position based on similarity values to adapt with moving the location of face parts in the image. Finally, the experimental results of the proposed approach were compared with many of approaches mentioned in related works.

4. The Proposed Face Recognition Approach

In this section, the proposed face recognition approach is presented and discussed in detail, which can be divided into four consecutive stages as shown in Figure 1. In the initial stage, the image will be enhanced using the prepressing techniques. In stage 2, the greedy search algorithm is employed to find the optimal landmark points in face parts found in face image in terms of the similarity between each landmark of a face image with the corresponding landmark in other face images of same face, this stage is thoroughly illustrated in Section 4.1. In the third stage, based on the optimal landmarks extracted by greedy search, the graph of the face image is created where the landmark points located in the background of the image will be exempted from sharing in the graph.

To perform the recognition process in the proposed approach, we prior fixed a number of landmark points in the face image and located them using the threshold stated in [5] to ensure that all landmark points are defined within the face involved in an image since the image contains parts of background. This stage is discussed in Section 4.2 In the final stage, the probe face images are recognized based on the EBGM technique where Eq. (2) plays the main role in the recognition of the graph nodes previously constructed. This stage is thoroughly described in Section 4.3. These stages of the proposed approach are thoroughly discussed with more details in the following subsections.

After the recognition process, the computed similarity values for reference images with the probe image are stored and sorted in the database where the reference image that achieves the largest similarity will be in rank one.

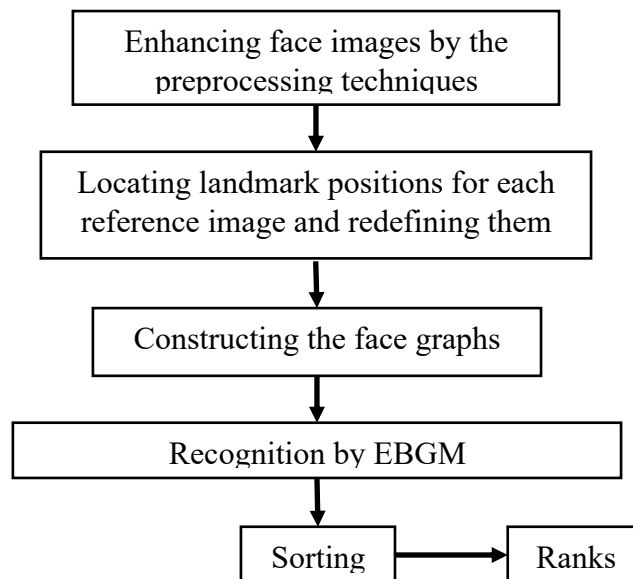


Fig. 1. Flowchart of the proposed face recognition approach

In the first step, the image information is restored from the image database to be enhanced using the Histogram Equalization and Median Filtering techniques to optimize the contrast levels and remove the noise. It should be noted, there are two types of images for each subject: one natural image (i.e., reference image) and set of images with variations such as occlusion (scarf and sunglasses), illumination and expression exploited to find the optimal landmark positions (i.e., model images), where each landmark point selected in reference image achieves the highest similarity value of five model images will be chosen in recognition stage. Figure 2 shows the reference and model images that are used in the proposed approach for all cases.

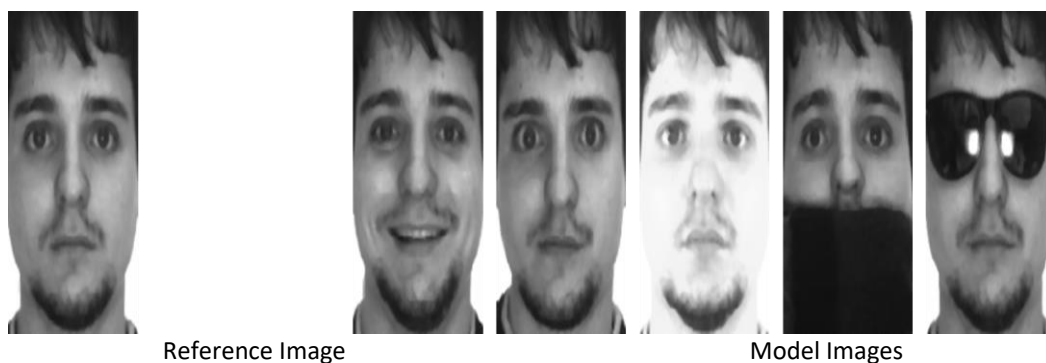


Fig. 2. Reference and model images that are used for all cases in the proposed approach

4.1 Definition of Landmark Positions for Images

The face graph is a set of pixel intensities located in face boundaries of image. The proposed approach is based on pixel intensities to perform the recognition process. The single probe image will be compared to all reference images stored in database to determine the similarity values based on the previously selected landmark points as illustrated in Figure 3.

Since the landmarks were used in the recognition process and some of them have more discriminatory than others. In each reference face image, the greedy search algorithm will be called to determine its optimal landmark positions according to the similarity value computed between the

landmark point of reference image and corresponding landmark point of model images to be exploited in the proposed approach.

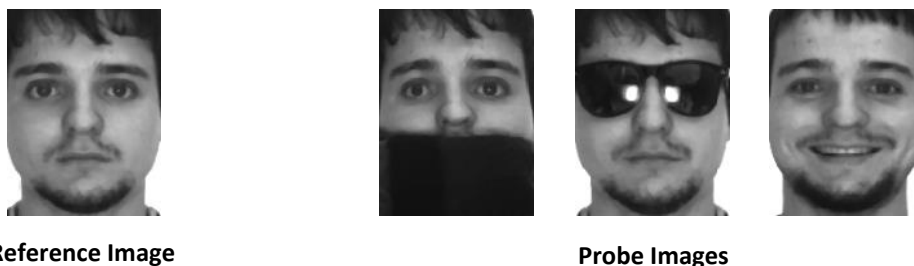


Fig. 3. Matching process of a reference face image with probe face images

Therefore, discriminatory landmarks have a key effect in the matching process between the given two face images which will eventually enhance the recognition accuracy [48]. Each landmark position will be represented in the x-axis and y-axis as shown in Figure 4b.

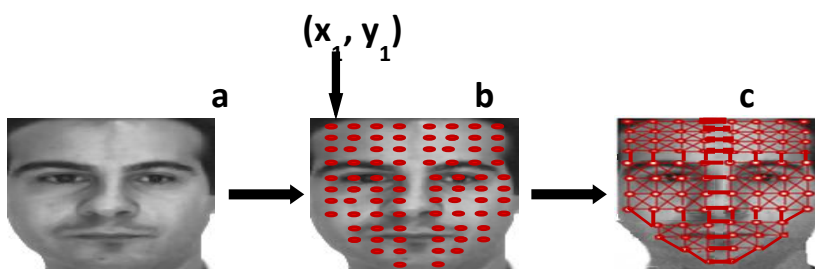


Fig. 4. Automatically selected facial landmark points for a face image [5]

In our approach, many face images were studied at first to define a number of landmarks that can be located surely within the face and not in the background of the image where they are located using the threshold stated in [5]. All face images share the same number of landmarks.

In the proposed approach, each reference and model image, such as the part of face image shown in Figure 5, has a size of 40×40 pixels and two optimal landmark point positions will be located in each 10×10 pixels of the face part involved in the image to ensure the landmark points will be distributed throughout the face; the two optimal landmark points are the optimal landmark point in one of face image and the corresponding landmark point in another face image and vice versa.

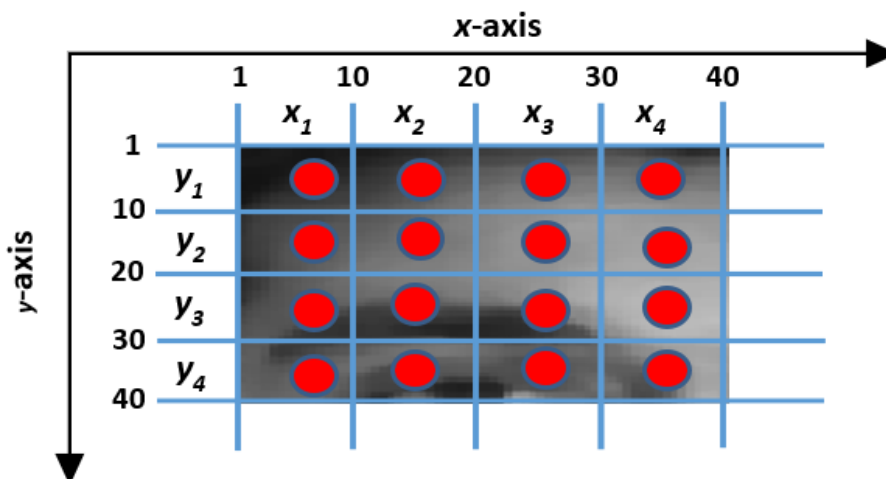


Fig. 5. Part of boundaries of generating landmarks in each face image

The optimal landmark point position has the best similarity value with the corresponding landmark point position of another face image. It should be noted the optimal landmark point and corresponding landmark points will be applied in reference and model images at the same time as shown in Algorithm 2.

Algorithm 2 Greedy Algorithm to Locate the Optimal Landmark Positions

Input: Pixel coordinates; Intensities of face image

Output: Optimal and corresponding landmark positions

```
1  for each_partitions(10×10 pixels) within face in image do
2    best_similarity_value = 0;
3    for each_model_image do
4      for j = 0 to ltrGreedy do
5        Select landmark_point randomly located within 10 × 10 pixels of current
6        face_of_image;
7        Build Complex_Jet_model of landmark_point for model image as shown
8        in Algorithm 3;
9        Build Complex_Jet_reference of landmark_point for reference image as
10       shown in Algorithm 3;
11       for landmark_point_position = landmark_point -1 to landmark_point +1
12       do
13         Build New_Complex_Jet_model of landmark_point_position for model
14         image as shown in Algorithm 3;
15         Build New_Complex_Jet_reference of landmark_point_position for
16         reference image as shown in Algorithm 3;
17         Calculate the average for new_similarity_value by
18         (Complex_Jet_model with New_Complex_Jet_reference) and
19         (New_Complex_Jet_model with Complex_Jet_reference) according to Eq. (3);
20         if new_similarity_value > best_similarity_value then
21           best_similarity_value = new_similarity_value;
22           Keep landmark_point;
23           Keep landmark_point_position;
24         end if
25       end for
26     end for
27   end for
28 end for
```

Therefore, the distribution covers the face without the background of the face image where around each optimal landmark point position located in each 10 × 10 pixels of the face image, a set of landmark points will be located. These landmark points have the best similarity values with the corresponding optimal landmark point of another face image. Also, the set of landmark points and corresponding landmark points will be applied for reference and model images at the same time. Therefore, the optimal landmark points will be in the reference image while the corresponding landmark points in the model image and vice versa.

Moreover, each face image is portioned into m portions along the x-axis and n portions along the y-axis. The range for each landmark is defined within a size of 10 × 10 pixels. Figure 5 depicts the process of creating many landmarks for a face image. According to the notion of permutation and

combination, the collection of all possible landmarks in each facial image is formed by $m \times n$ matrix as shown in Figure 4b, where the Landmark Points (LP) are obtained from the face image as shown in Eq. (1). Therefore, the proposed approach is based on a fixed number of optimal landmark points for each face image to make the matching process more accurate.

Figure 4b shows the distribution of the optimal landmark points within the face boundaries where each one point will be in one of 10×10 pixels. Determining the optimal landmark point positions within 10×10 pixels will be using the greedy algorithm as shown in Algorithm 2.

The proposed approach calculates the similarity of the current landmark point of a face image with a corresponding landmark point in another face image independently of other selected landmark points. Therefore, the calculation of similarity is based on the nearest neighbouring pixels of the candidate landmark point.

As previously stated in Section 2.2, the greedy algorithm is a heuristic that can be used for optimization problems. It usually starts with an initial solution and keeps the current best solution until the best new solution is founded. Therefore, the greedy algorithm searches for a better solution in the neighbourhood. If a better solution is founded, it changes the current solution with it. The termination condition is based on a number of iterations or meeting the goal [49].

In the greedy algorithm to locate the optimal landmark positions, all face images will share the same number of refined landmark points selected within the face boundary. Since, a number of portions (10×10 pixels) contain a background of the face images, as shown in Figure 4a, so that the number of the portions which contain the optimal landmarks were selected in the initial step of the proposed approach as shown in Figure 4b. Then, the best similarities will be calculated according to Eq. (3) to refine each landmark point within its boundary.

The proposed approach can be described as a dynamic approach since it searches to locate the corresponding landmark point for a specific landmark point in the same location (x, y) of that landmark point in the corresponding face image and it searches within the area selected from $(x-1, y-1)$ to $(x+1, y+1)$ as shown in Line 7 of Algorithm 2. The following steps describe the greedy algorithm to locate the optimal landmark positions, as shown in Algorithm 2:

- i. **Step 1:** Select the number of portions of face image to ensure landmark points are located within the face image and not in the background of the image. Since a number of portions of the face image of the AR dataset can involve a background rather than the face as shown in Figure 4a.
- ii. **Step 2:** In each portion of the face image, one landmark point denoted by *landmark_point* is selected randomly in each iteration of the greedy algorithm to decide the landmark point which has the best similarity of all model images within same the portion as shown in Line 3 and 4.
- iii. **Step 3:** Build the jet matrix for selected landmark points of model and reference face images as shown in Lines 6, 7, 9 and 10 of Algorithm 2.
- iv. **Step 4:** Search for the optimal landmark points in model and reference images by finding the best similarities denoted by *best_similarity_value* of the jet matrix which is built-in Step 3 of landmark points and selected in Step 2.
- v. **Step 5:** Store the landmark points and the corresponding landmark points denoted by *landmark_point* and *landmark_point_position* respectively which achieve the best similarities as shown in Lines 14 and 15.

Algorithm 3 shows the algorithm used to create the jet for landmark points using Gabor wavelet. Since the intensity value of the pixel of the face image plays the main role in the EBGM technique to

achieve the recognition process, the jet algorithm fetches the intensity value of the pixel of face images as shown in Algorithm 3. Then, the neighbouring pixel intensity values for selected landmark points of reference and model images as shown in Algorithm 3 are stored in matrices as shown in Line 1 and 2 of Algorithm 3. Whereas the intensity value of pixels that is out of face image boundary will be assigned to 0. Finally, the mathematical calculation of Gabor Wavelet according to EBGGM algorithm which includes convolution technique for pixel intensity values and Gabor Wavelet is shown in Line 3 and 4 of Algorithm 3. The Gabor Wavelet transform is based on Frequencies (Fr) and Orientations (Or). Therefore, a total of $Fr \times Or$ complex coefficients is generated for each landmark point to produce the Jet vector of length $Fr \times Or$ after the convolution process. The Jet vector is represented by a total of $Fr \times Or$ magnitude values and a total of $Fr \times Or$ phase θ .

Algorithm 3 Jet Algorithm to Create Complex Jet of the Landmark Point

Input: Landmark point; Matrix size for landmark points located around that landmark point; Intensities of points defined in the matrix

Output: Jet matrices of the given landmark point and corresponding landmark point

1 Define the size of the matrix which are denoted as x_vector and y_vector around the selected landmark points, denoted as x_value and y_value , and fetch the pixel intensity values of probe and reference face images to $Intensity_from_Reference_Image$ and $Intensity_from_Probe_Image$ matrices.

2 Fill intensity values of pixels which are around the selected landmark points in $Intensity_LandPoint_RefImg$ and $Intensity_LandPoint_Mdllmg$ matrices. If the point is out of the face image boundary, the intensity value is zero.

3 Define the frequencies and orientations for the Gabor wavelet. Then build the Gabor wavelet matrix to be used as a mask based on frequencies and orientations values.

4 Apply the convolution process for $Intensity_LandPoint_RefImg$ and $Intensity_LandPoint_Mdllmg$ matrices with Gabor wavelet matrix. The jet denoted by Jet_Ref and Jet_Mdl of selected landmark point contains $Fr \times Or$ magnitude values and a total of $Fr \times Or$ phase θ after achieving the convolution process. Finally, Jet_RefImg_Matrix and Jet_Mdllmg_Matrix represents the total jet based on Fr and Or of Gabor wavelet and x_vector and y_vector .

In Algorithm 2 the best similarity values of landmark points are calculated to find the corresponding landmark points. As noted previously, the EBGGM technique employs the selected landmark points in the recognition phase. The selected landmark points are the optimal landmark points located in 10×10 pixels of the face image.

4.2 Creation of Face Graph

The optimal landmark and corresponding landmark are found by the greedy algorithm as shown in the previous subsection for each 10×10 pixels in both reference and model images. The proposed approach takes to account that all face images should share the same number of optimal landmark points selected within the face boundary to obtain more accurate in recognition process.

The validation scheme is illustrated in Figure 4c where facial landmark points that are not located within the face are initially eliminated. A face graph is created for each face image using the optimal landmark located in each 10×10 pixels found by the greedy algorithm which finds corresponding landmark points of the face graph of another face image by computing the maximum similarity. Each facial portion of 10×10 pixels contains optimal facial landmarks $y = (\text{optimal point, corresponding$

point) where y is used to generating the graph of each face. The solution y is mapped into the LP matrix as shown in Eq. (4). The LP matrix will be applied to the face image as shown in Figure 4c. Each point in LP is a portion that contains the two optimal landmarks in the graph. The landmark nodes located in Algorithm 2 by calculating maximum similarity have edges to be fully connected. Moreover, the Jet vector of each node within 10×10 pixels is calculated as discussed in Eq. (4). The proposed model of landmarks of reference and model images that achieve maximum similarity will be used in the recognition process as shown in the next subsection. The test face image needs to be recognized (probe image) where the LP will be used to construct the face graphs for the probe image.

$$LP = \begin{pmatrix} y_{11} & y_{12} & \cdots & y_{1n} \\ y_{21} & y_{22} & \cdots & y_{2n} \\ \vdots & \vdots & \vdots & \vdots \\ y_{m1} & y_{m2} & \cdots & y_{mn} \end{pmatrix} \quad (4)$$

Where LP matrix components represent the landmark points inside a specific face in image. For example, the element y_{11} represents the optimal landmark and corresponding landmark points within range (0, 10) where Gabor wavelet transform was computed for each landmark point in the LP matrix.

4.3 Recognition

Two graphs are formed by optimal landmarks and the corresponding landmarks. The two graphs are applied for probe and reference images. The similarity between each node in the graph of the reference image and the corresponding node in the graph of the probe image is computed using Eq. (3). In the proposed approach each point in the graph is based on neighbouring nodes in the face image to build a complex jet and calculating the similarity.

It is worth noting that the proposed approach converts initially the occluded portion of the face image to a black block to be able to handle them. Where the parts of real occlusions are defined by changes unexpected in pixel intensities as stated in [5]. The proposed approach manipulates the occluded portions of the face image by discarding them. Regarding the optimal points and corresponding points which have occluded points (black points) or points located out of boundary of face image in their jets, they will be assigned to value zero in calculating the similarity values.

The proposed approach is based on the similarity values between *Optimal_landmark* and *Corspnd_optimal_landmark* points previously located in reference and model graphs. In the recognition process, the similarity values between *Optimal_landmark* and *Corspnd_optimal_landmark* points of reference and probe graphs will be recomputed by Eq. (3). Where the average similarity for each node S_{node} in graph is calculated as shown in Eq. (5). Algorithm 5 shows the steps of recognition process.

$$S_{node} = \frac{1}{x \times y} \sum_{j=1}^{x \times y} S(J_j, J'_j) \quad (5)$$

Where $x \times y$ is the number of neighbouring nodes in the face image for node n of graph, J_j is a jet of the node in a graph of reference image, J'_j is a jet of the node in a graph of probe image, $S(J_j, J'_j)$ is the similarity value computed by Eq. (3) between J_j and J'_j , and j is the current neighbouring node for node n .

Algorithm 4 Similarity_Computation_Algorithm (*point1*, *point2*)

Input: Two landmark points; Intensities of the two points; Intensities of neighbouring points for each of them

Output: The similarity value between the two landmark points

- 1 Build *Probe_Jet1* of *point1* of probe image as shown in Algorithm 3;
- 2 Build *Reference_Jet1* of *point1* of reference image as shown in Algorithm 3;
- 3 Build *Probe_Jet2* of *point2* of probe image as shown in Algorithm 3;
- 4 Build *Reference_Jet2* of *point2* of reference image as shown in Algorithm 3;
- 5 Calculate the *similarity_value1* between *Probe_Jet1* and *Reference_Jet2* according to Eq. (3);
- 6 Calculate the *similarity_value2* between *Reference_Jet1* and *Probe_Jet2* according to Eq. (3);
- 7 Return (*new_similarity_value1* + *new_similarity_value2*) / 2;

Algorithm 5 Recognition Phase

Input: Optimal and corresponding landmarks; Pixel coordinates; Intensities in each face image

Output: The similarity value between the probe and reference images

- For each image *num_image* stored in the database, fetch the optimal landmark points and corresponding points to *Optimal_landmark* and *Corspnd_optimal_landmark* founded in Section 4.1 respectively.
- 1
 - 2 For each graph *graph* and landmark points selected in *graph*, calculate *best_similarity_value* based on Algorithm 4.
Calculate *sum_similarity_of_graph* by *best_similarity_value* values for points in LP matrix then calculate the average similarity for whole face image which is denoted by *average_similarity_for_graphs*.
 - 3

The overall average similarity for the entire face image (ES) is computed as in Eq. (6).

$$ES = \frac{1}{m \times n} \sum_{y=1}^{m \times n} S_{node} (J_y, J'_y) \quad (6)$$

Where $m \times n$ is the number of nodes in the LP matrix, $S_{node} (J_y, J'_y)$ is the similarity computed in Eq. (5) from optimal and corresponding landmarks for node y , and y is the current node n . Finally, the reference image that achieves maximum overall average similarity with the probe image will be the target result. Therefore, the overall average similarity for all reference images is ranked in descending order and then the reference image with the largest similarity value is in rank number one.

5. Experimental Results

This section presents the experimental results obtained using the proposed approach that were customized to recognize faces under occlusions and variations. Also, the proposed approach is compared with other approaches. This section starts by describing the experimental environment in Section 5.1. In this subsection, details are presented about the results of the comparative approach, and datasets that were used in the experiments. Finally, the experimental results are presented and compared with the other mentioned approaches against the occlusion challenge and several variations in Section 5.2.

5.1 Experimental Environment

In this section, the effectiveness of the proposed approach is evaluated. For evaluation purposes, the experimental testing platform for the proposed approach was performed on a 2.53 GHz CPU Desktop with 3GB RAM and the programming language is C# windows on Microsoft Visual Studio 2010. The datasets that have been used in our experiments are the face image AR dataset [29] and a new dataset proposed in this paper, that we have created by modifying the AR dataset through adding synthetic occlusion blocks of different sizes where we called it “modified AR”.

This research work has been carried out by taking into account face recognition under many cases including controlled/ideal condition, partially occluded condition, different facial expressions, and different lighting condition as done by other comparative approaches such as Line Edge Map (LEM) [36] Elastic Bunch Graph Matching (EBGM) [20], Adaptively Weighted Patch Pseudo Zernike Moment (AWPPZMA) [38], Adaptively Weighted Sub-Gabor Array (AWSGA) [16], Psychophysically Inspired Similarity Mapping (PISMA) [8], Ensemble String Matching (ESM) [40], Harmony Search Oriented-EBGM (HSO-EBGM) [5]. And Gabor-High Dimensional Local Binary Patterns + Membrane Inspired Binary Bat Algorithm (Gabor-HDLBP+MIBBA) [9].

The AR dataset contains more than 4000 frontal colour images for 126 persons (70 male and 56 female). Each person subject consists of 26 images captured in two separate sessions by two weeks intervals. Face images are subject to varying occlusions (sunglasses and scarf), facial expressions (smile, anger, or scream), and illumination conditions (left light on, right light on, and both lights on). The face images of 100 subjects (50 male and 50 female) involving all variations were used in our experiments.

In all the experiments, images were enhanced and normalized with classical preprocessing techniques (i.e., median filtering and histogram equalization) and then cropped. The resolution of the pre-processed and cropped images is 80×120 pixels. Figure 6 illustrates instances of face images from the AR dataset. We added new modifications to AR dataset by removing blocks of pixels as shown in (M), (N), (O), and (P) of Figure 6. The modifications were conducted on neutral face under controlled conditions from session 1 including removing 30×30 , 50×50 , 70×70 , and 100×100 pixels, respectively.

A detailed explanation is shown for the experimental results that are obtained by the proposed approach which shows its outperformance against the results by other existing face recognition approaches in the literature.

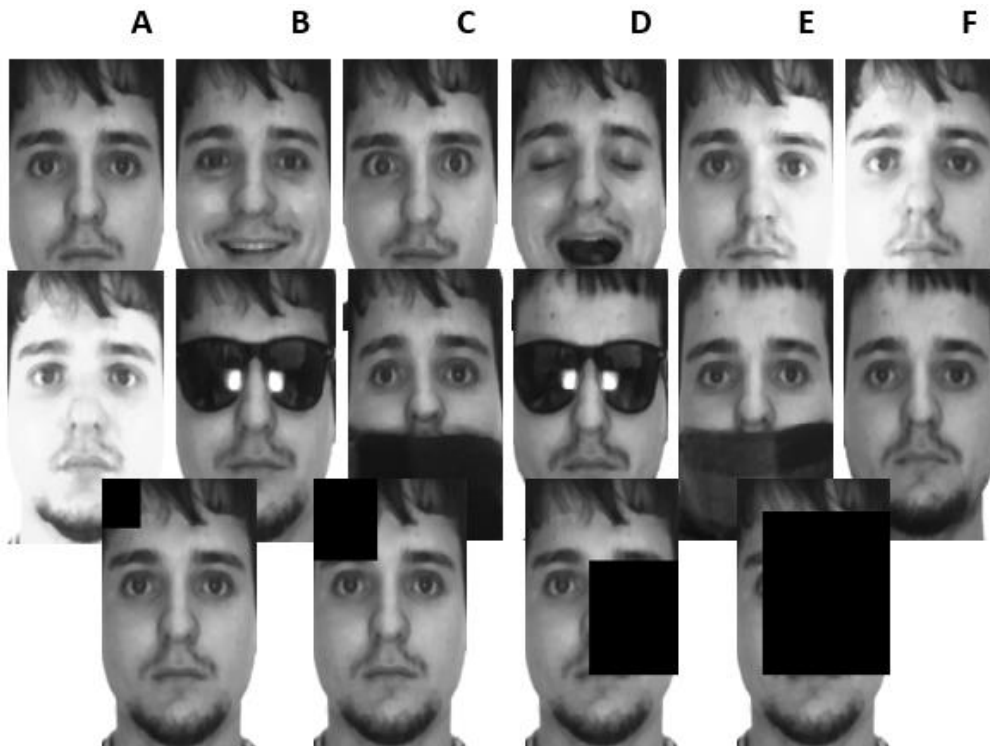


Fig. 6. Samples of AR face images for one subject (the subject is a set of face images in several cases for the same person). (A) is a neutral face under controlled conditions from session 1; (B), (C), and (D) are faces with smile, anger, and scream expressions respectively from session 1; (E), (F), and (G) are faces under varying light conditions from session 1; (H) and (I) are partially occluded faces with sunglasses and scarf respectively from session 1; (J) and (K) are partially occluded faces with sunglasses and scarf respectively from session 2; (L) is a neutral face under controlled conditions from session 2. (M), (N), (O), and (P) are synthetically occluded faces by removing 30×30, 50×50, 70×70, and 100×100 pixels, respectively

5.2 Comparative Evaluation

To validate the performance of the proposed approach, the best average recognition rates obtained from our proposed approach are compared with other well-known approaches abbreviated and summarized in Table 1. These approaches produced the best-known results which are recorded previously for the AR dataset and some of these approaches had been applied to the modified AR dataset after implementing these approaches. Some of these approaches used EBGM as a primary technique to recognize faces of AR dataset and others used hybrid technique designed especially for recognizing faces. It is noteworthy that real occlusions (scarves and sunglasses) and synthetic occlusions are discarded by the proposed approach. Where the parts of real occlusions are defined by unexpected changes of pixel intensities as stated in [5].

Table 1
 The abbreviations for the comparative approaches

Abbreviation	Comparative Approach	Reference
LEM	Line Edge Map	[37]
EBGM	Elastic Bunch Graph Matching	[20]
AWPPZMA	Adaptively Weighted Patch Pseudo Zernike Moment	[39]
AWSGA	Adaptively Weighted Sub-Gabor Array	[16]
PISMA	Psychophysically Inspired Similarity Mapping	[8]

ESM	Ensemble String Matching	[40]
HSO-EBGM	Harmony Search Oriented-EBGM	[5]
Gabor-HDLBP + MIBBA	Gabor-High Dimensional Local Binary Patterns + Membrane Inspired Binary Bat Algorithm	[9]

The comparative results of the recognition rates are recorded in Table 2. These results are obtained by the proposed approach, which are compared with those obtained by the other comparative approaches. The results shown in Table 2 to Table 7 refer to the average recognition rates of all approaches. The average recognition rates of the proposed approach are obtained by 30 runs executed for each experiment. The best recognition rates (the largest value is the best) are highlighted in bold font. The mark '-NA-' in the table refers to the corresponding approach that did not experiment with such dataset or that its results are unknown.

5.2.1 Recognition Rates of Faces with Ideal Conditions

We evaluate the proposed approach under relatively controlled conditions on AR and modified AR datasets. The recognition rates of the proposed approach are compared with those of Gabor-HDLBP + MIBBA, HSO-EBGM, ESM, AWPPZMA, LEM, and EBGM approaches, as shown in Table 2 to Table 7. The best recognition rates are highlighted in bold. The neutral face from session 1 (e.g., Figure 6 (a)) is defined as a reference, and the neutral face from session 2 (e.g., Figure 6 (l)) is defined as the probe image. Table 2 shows that the proposed approach outperformed the HSO-EBGM, EBGM, and AWPPZMA approaches and it showed comparable recognition performance on par with ESM, Gabor-HDLBP + MIBBA, and LEM approaches on the AR dataset because the proposed approach can adapt with changes of the face parts of different images for the same person by searching for corresponding landmarks in the same location of optimal landmarks and around optimal landmarks. However, Gabor-HDLBP + MIBBA achieves the best recognition rate, then the proposed approach on the AR dataset. The proposed approach can treat the changes in parts of the face of different images for the same person, because of the shortcomings of the classical EBGM in dealing with this challenge. Thus, the possibility of addressing this challenge remains limited. Finally, in the modified AR dataset, the neutral face (Figure 6 (a)) is defined as a reference and the synthetically occluded faces (Figure 6 (m)-(p)) is defined as the probe images. The proposed approach outperformed the HSO-EBGM and EBGM approaches using the modified AR dataset for all occlusion sizes because the synthetic occlusions are discarded where if a small number of landmarks located out of occlusions can achieve the good similarity, which is enough to recognize faces. It can be noted that the results of HSO-EBGM and EBGM approaches that are shown in Table 2 are collapsed gradually based on increasing occlusion size because these approaches compute the average of similarity values of all landmarks to define the recognition rates where the number of landmarks which achieve the bad similarity is increased with increasing the occlusion size.

It is observed from the average recognition rates shown in Table 2 for the modified AR dataset, the proposed approach remains almost the same using varying occlusion sizes when the synthetic occlusions are discarded because the small number of optimal landmarks is enough to perform the recognition process.

Table 2
 Comparative performance in terms of the average recognition rate with controlled/ideal conditions

Approach	Average Recognition Rate (%)				
	AR Dataset	Modified AR Dataset - Occlusion Size			
		30×30	50×50	70×70	100×100
HSO-EBGM	94.1	98	77.4	64.8	51.3
EBGM	84	73	42	22	8
ESM	96.58	-NA-	-NA-	-NA-	-NA-
AWPPZMA	92.31	-NA-	-NA-	-NA-	-NA-
LEM	96.58	-NA-	-NA-	-NA-	-NA-
Gabor-HDLBP + MIBBA	98	-NA-	-NA-	-NA-	-NA-
Proposed Approach	97.1	99.1	98.8	98.7	98.5

5.2.2 Recognition rates of faces with realistic partial occlusions

In general, the realistic occlusions degrade the performance of recognition systems where it is not realistic to deal with them as another part of the face, such as eyes, nose, lips, etc. The proposed approach converts the realistic occlusions to black blocks since they can be defined in the initial step by unexpected changes of pixel intensities then the proposed approach will discard them. In this section, the performance of proposed approach using realistic partial occlusions (sunglasses and scarves) is presented.

The neutral face (Figure 6 (a)) is used as a reference image while four occluded faces with sunglasses and scarf from session one and session two (Figure 6 (h)-(k)) are used as the probe images. The average recognition rates of the proposed approach and other approaches are presented in Table 3.

The best recognition rate is highlighted in bold. It can be seen from Table 3 that the proposed approach is significantly outperformed the other approaches in partial occlusion of session 1 since the model images used to construct the graphs of face image are taken from the same session.

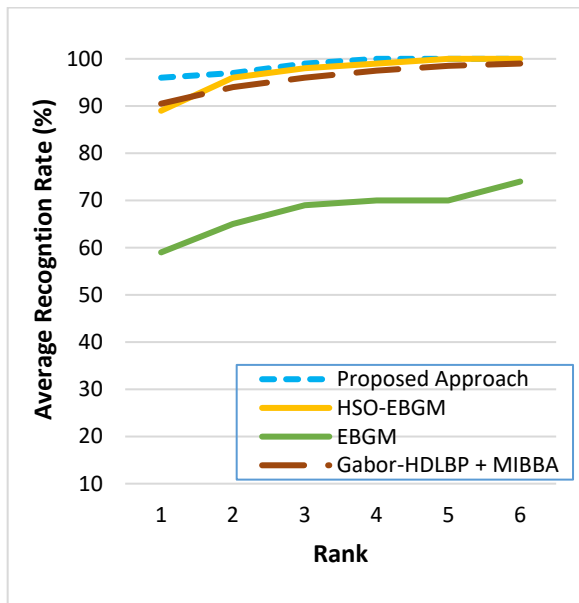
Table 3
 Comparative performance in terms of the average recognition rate with real occlusions

Approach	Average Recognition Rate (%)				Average Recognition Rate (%) of Both Sessions
	Session-1		Session-2		
	Sunglasses	Scarf	Sunglasses	Scarf	
HSO-EBGM	88.20	91.8	80	83.3	85.83
EBGM	57	40	33	27	36
ESM	87.18	94.87	76.07	88.3	86.54
PISMA	78	79	55	49	65.75
AWSGA	38	84	20	70	53
Gabor-HDLBP + MIBBA	90.56	94	72	94.06	87.65
Proposed Approach	96	98.5	83.2	85.3	90.75

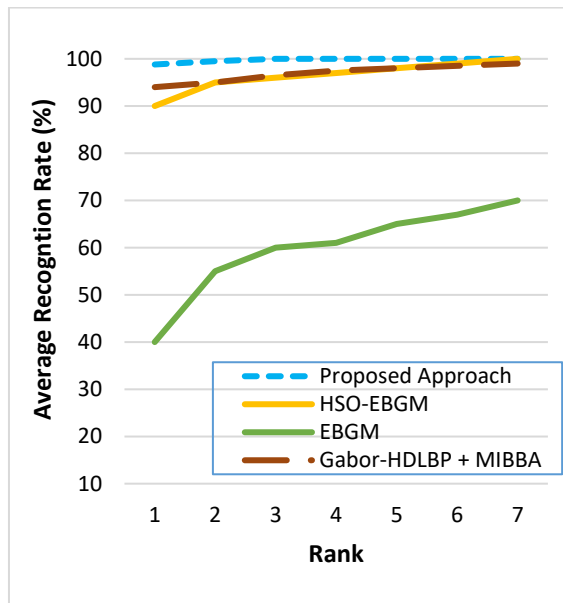
Moreover, the proposed approach achieves an average recognition rate in partial occlusion of session 2 comparable to HSO-EBGM, Gabor-HDLBP + MIBBA, and ESM which are the standard approaches to handle the partial occlusion. This is due to the proposed approach define the optimal landmarks dynamically through searching to the corresponding landmarks around the optimal landmarks to achieve larger similarity.

These results show the ability of the proposed approach to handle partial occlusions and hence able to recognize partially occluded faces.

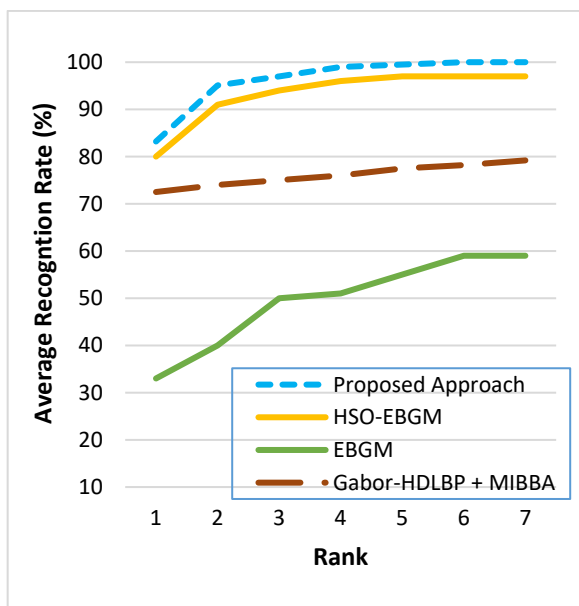
Figure 7 shows the average recognition rate of the proposed approach, EBGM, HSO-EBGM and Gabor-HDLBP + MIBBA regarding the Cumulative Match Characteristics (CMC) curve. As shown by the results in Figure 7, the proposed approach reaches about a 100% recognition rate within ranks two and five, respectively, in all the occlusion cases, in indication for its superiority in manipulating occlusions, since it utilizes the best landmarks for recognition process.



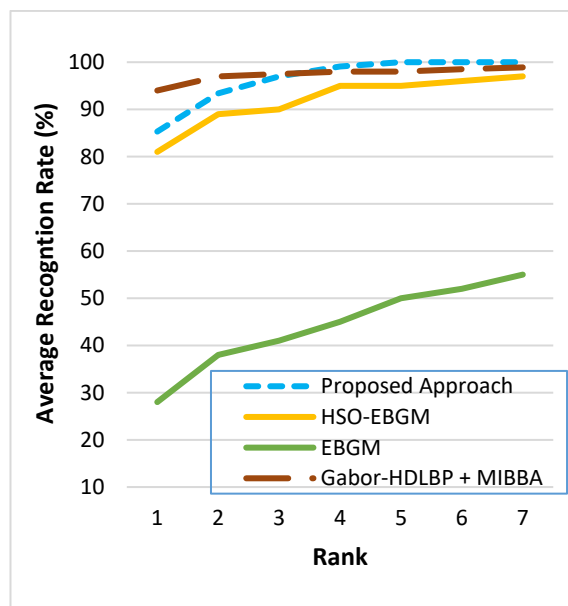
(a) Sunglasses Session 1



(b) Scarf Session 1



(c) Sunglasses Session 2



(d) Scarf Session 2

Fig. 7. The average recognition rate of the proposed approach using partially occluded faces of AR dataset in terms of cumulative match characteristic graphs

5.2.3 Recognition rates of faces with facial expression variations

Changes produced by facial expression can be one of the common main factors that could affect the performance of face recognition techniques. To evaluate the performance of the proposed approach on different facial expressions (smiling, angry, and screaming), experiments have been performed using facial expressions of session 1 and session 2 of the AR dataset [50].

In the experiment of a face image with neutral expression in session 1 (Figure 6 (a)) it has been used as a reference image while the face images with three different expressions (Figure 6 (b)-(d)) from the same session have been used as the probe images.

Table 4 shows the experimental results of the proposed approach and other approaches using varying facial expressions from Session 1. The best recognition rates are highlighted in bold.

According to the results of Table 4, it can be observed that Gabor-HDLBP + MIBBA approach achieves the best average recognition rate, then the proposed approach, where the proposed approach outperforms the other approaches, these results show the robustness of the proposed approach since it is designed to adapt with changing the parts of face images by utilizing the similarity of each optimal landmark in the recognition process.

Also, since the scream expression dropped the recognition rates of the proposed approach to about 66%, the proposed approach is affected. An indication that the scream expression can give more impact on the recognition accuracies than soft expressions such as anger and smile as shown by results since the scream expression contains large changes in locations of optimal and corresponding landmarks in probe face images where the proposed approach can handle a limited part of these changes.

From Table 4, it can be seen that the proposed approach is comparable and better recognition rate on par with HSO-EBGM, AWPPZMA, and AWSGA, LEM approaches and they significantly outperform the EBGM and ESM for all cases, because the proposed approach determines the optimal landmarks by searching to corresponding landmarks around the optimal landmarks to achieve larger similarity where this can enhance the adaption with changes of face parts.

Table 4
 Comparative performance in terms of the average recognition rate under varying facial Expressions (Session 1)

Approach	Average Recognition Rate (%)			
	Smiling	Anger	Scream	Average
HSO-EBGM	93.6	95	53.4	80.7
EBGM	74	88	29	63.7
ESM	85.47	87.18	26.49	72.36
AWPPZMA	96.58	87.18	38.46	74.7
LEM	79.49	93.16	31.62	68.09
AWSGA	95.72	94.87	33.33	74.64
Gabor-HDLBP + MIBBA	-NA-	-NA-	-NA-	97.6
Proposed Approach	98.4	96.7	66.3	87.13

The Gabor-HDLBP + MIBBA approach achieves the best average recognition rate, then the proposed approach because the expression variations effect on local parts of faces, where EBGM cannot adapt significantly to the changes resulting from expressions, despite the proposed approach based on the classical EBGM in determining the landmark points, the proposed approach adapt to a limited extent with changes of face parts of the probe face images by finding the landmark points that give the greatest similarity with the corresponding landmark points in the reference image.

Figure 8 shows the average recognition rate of the proposed approach and HSO-EBGM with different ranks in terms of the Cumulative Match Characteristics (CMC) curve where the rank represents that the required image which satisfies the probe image is defined within the selected rank. The proposed approach achieves the 100% average recognition rate in rank five against anger whereas it achieves 100% average recognition rate in rank two against smiling because the model image used to find the optimal landmarks is same for probe images. Regarding the scream case which demonstrates larger shifting for face parts, the proposed approach achieves about 100% average recognition rate in rank ten.

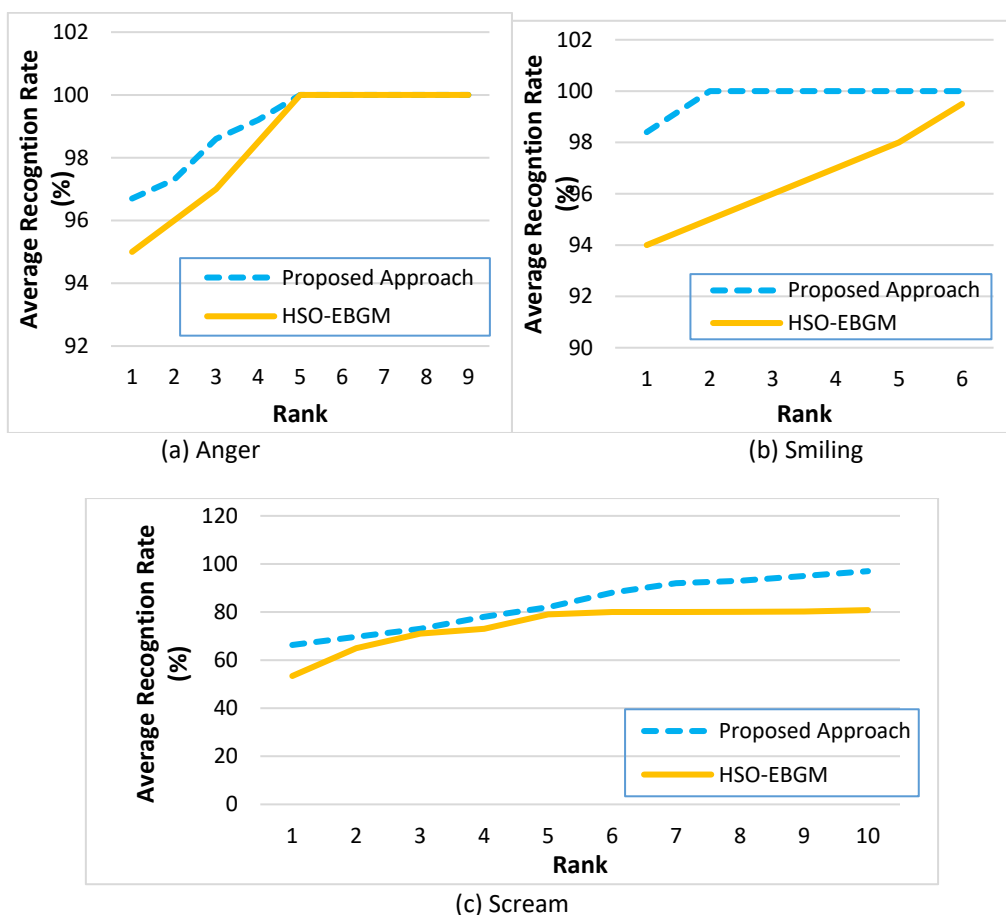


Fig. 8. The average recognition rate of proposed approach using face expressions of AR dataset in terms of cumulative match characteristic graphs

The face image with neutral expression in session 1 (e.g., Figure 6 (a)) has been used as a reference image while the face images with three different expressions (e.g., Figure 9 (a)-(c)) from session 2 have been employed as the probe images. The experimental results of the proposed approach and the other approaches using varying facial expressions from Session 2 are tabulated in Table 5. The best recognition rates are highlighted in bold.

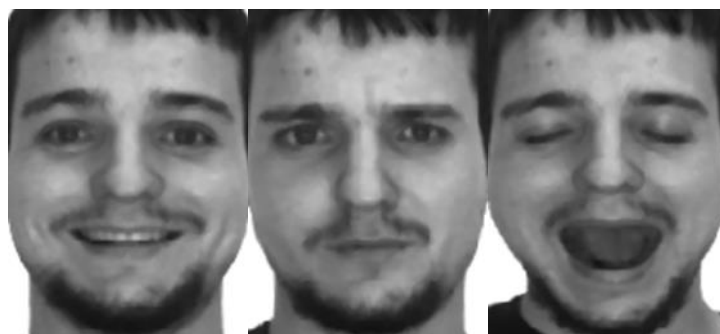


Fig. 9. Samples of AR face images for one subject (the subject is a collection of face images in different cases for the same individual) with facial expressions from session 2. (A) Smile (B) Anger, and (C) Scream

It can be seen from Table 5 that the proposed approach significantly outperforms the EBGM and HSO-EBGM in smiling and anger cases. Also, proposed approach achieves a better recognition rate than EBGM and HSO-EBGM in the case of the scream image, since the proposed approach allow the optimal landmarks locating corresponding landmarks around the optimal landmarks. This enhances the possibility to achieve larger similarity. In general, the proposed approach stands next to the Gabor-HDLBP + MIBBA against the best average recognition rate of facial expression of session 2. Considering the results seen in Table 4 and Table 5, it is evident that the proposed approach shows comparable recognition performance with Gabor-HDLBP + MIBBA in smiling and anger cases on session 1 and session 2. Also, it can be observed that the average recognition accuracy of the proposed approach for anger expression in Table 4 approximately increases by 3 % compared to anger expression in Table 5 due to the reference images and probe images were taken from the same session for the results shown in Table 4 while the probe images used to compute the results shown in Table 5 were extracted from session 2 where the variations have increased since session 2 images were captured after a two-week time interval.

Table 5

Comparative performance in terms of the average recognition rate under varying facial expressions (Session 2)

Approach	Average Recognition Rate (%)			
	Smiling	Anger	Scream	Average
HSO-EBGM	86	86.2	46	72.73
EBGM	60	66	18	48
Gabor-HDLBP + MIBBA	-NA-	-NA-	-NA-	96.2
Proposed Approach	95.3	93.4	55.1	81.26

5.2.4 Recognition rates of faces with the illumination challenge

Illumination is one of the real challenges used to evaluate any face recognition system. In this subsection, the sensitivity of the proposed approach to illumination variations (left light on, right light on, and both light on) is evaluated on session 1 and session 2 of the AR dataset.

In the experiment, the neutral image in the AR dataset taken from session 1, as shown in Figure 6 (a), was selected as a reference image. The face images under three different lighting conditions, as shown in Figure 6 (e)-(g), taken from the same session were employed as probe images. The

average recognition rates of the proposed approach and the other approach are presented in Table 6, where the best recognition rate is highlighted in bold.

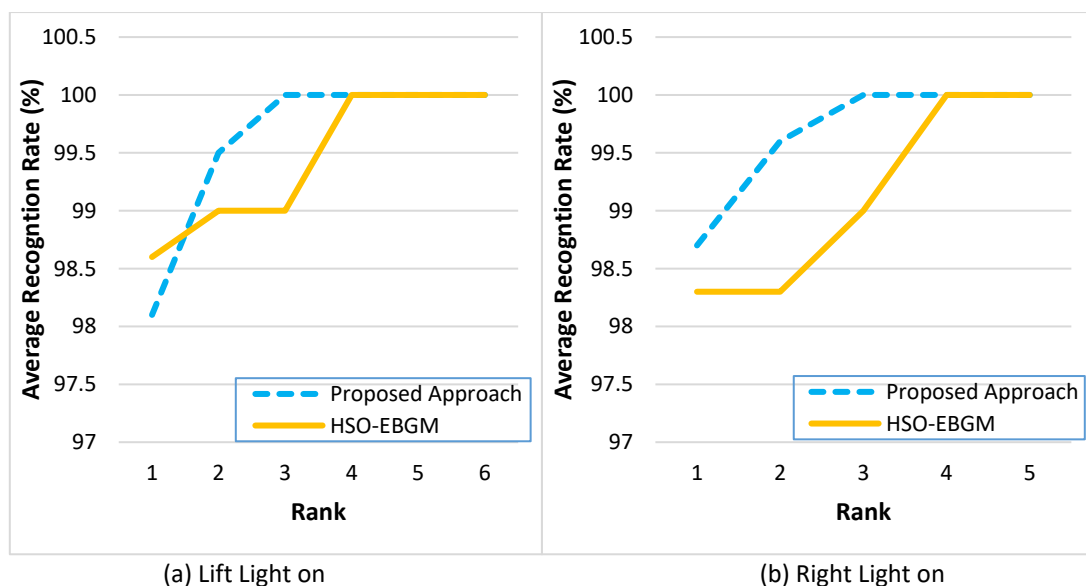
It can be noted from Table 6 that the proposed approach outperforms other approaches since it utilizes the similarity of optimal landmarks where changing the locations of landmarks and corresponding landmarks can decrease the effecting of illumination challenges. Further, the proposed approach can recognize faces by handling each optimal landmark independently from other optimal landmarks where a small part of optimal points which are located out of the affected blocks of face image can achieve good average recognition rate.

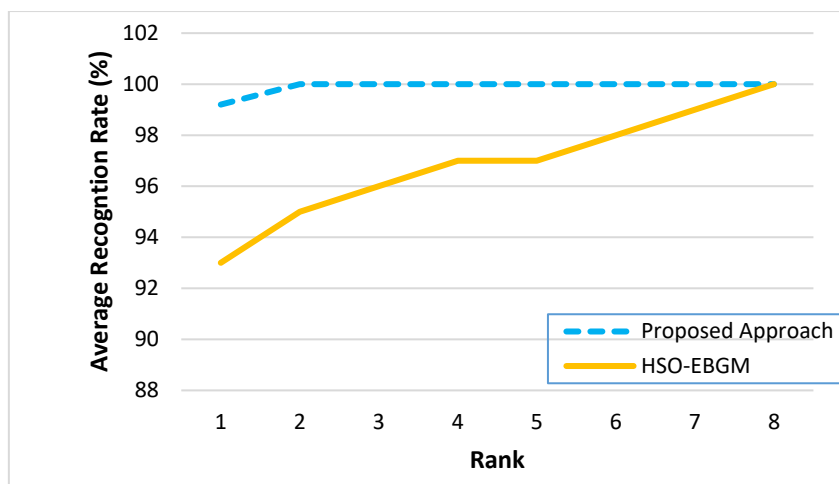
Whereas proposed approach achieves comparable recognition rates on par with HSO-EBGM, ESM, and LEM approaches, where LEM approach is one of the considerable illumination insensitive approaches, under different lighting conditions. This is because a part of located optimal landmarks achieves a good similarity in the recognition process since the corresponding landmarks are located around the optimal landmarks.

Table 6
 Comparative performance in terms of the average recognition rate under varying lighting conditions (Session 1)

Approach	Average Recognition Rate (%)			
	Left light on	Right light on	Both lights on	Average
HSO-EBGM	98.6	98.3	93	96.63
EBGM	93	89	78	86
ESM	94.02	94.02	73.5	87.18
AWPPZMA	74.36	64.96	42.74	60.69
LEM	92.31	91.45	73.50	85.75
AWSGA	23.93	5.98	23.8	17.9
Gabor-HDLBP + MIBBA	-NA-	-NA-	-NA-	99
Proposed Approach	98.1	98.7	99.2	98.66

As presented by the CMC graphs in Figure 10, the proposed approach reaches to 100% recognition rate in rank three whereas HSO-EBGM reaches in rank four to 100% recognition rate against the left and right light on, since the proposed approach is based on similarity of optimal landmarks, for all lighting cases.





(c) Both Light on

Fig. 10. The average recognition rate of proposed approach using varying lighting conditions of AR dataset in terms of cumulative match characteristic graphs

The neutral images in the AR dataset taken from session 1, as shown in Figure 6 (a), is selected as a reference image while the face images under three different lighting conditions, as shown in Figure 11 (a)-(c), taken from session 2 were employed as probe images. Table 7 shows the average recognition rate of the proposed approach and other approach using varying lighting conditions from session 2 where the best average recognition rate is highlighted in bold.

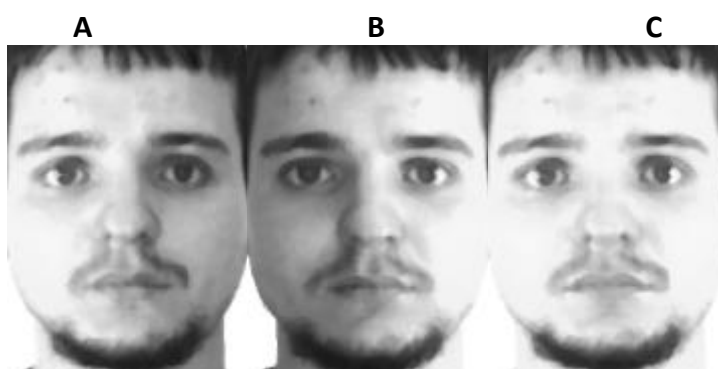


Fig. 11. Samples of AR face images for one subject (set of face images in different cases for the same individual) under different lighting conditions from session 2: (A) Left light on, (B) Right light on, and (C) Both lights on

It can be noted from Table 7 that the Gabor-HDLBP + MIBBA approach achieves a better average recognition rate than the proposed approach. Also, the proposed approach outperforms HSO-EBGM and EBGM approaches, since the proposed approach adapt with different lighting conditions by achieving high similarity between the optimal landmarks and corresponding landmarks located around optimal landmarks although the sensitivity of classical EBGM for illumination challenges.

Table 7
 Comparative performance in terms of the average recognition rate under varying lighting conditions (Session 2)

Approach	Average Recognition Rate (%)			
	Left light on	Right light on	Both lights on	Average
HSO-EBGM	91	92	94.3	92.43
EBGM	86	84.7	70	80.23
Gabor-HDLBP + MIBBA	-NA-	-NA-	-NA-	99
Proposed Approach	93.5	93.1	96	94.2

Therefore, the average recognition rate of the proposed approach for left light on and both lights on for session 1 as shown in Table 6 approximately increases by 4.6% and 3.2% respectively compared to left light on and both lights on for session 2 as shown in Table 7, because the reference image and probe images were taken from the same session for the results presented in Table 6 while the probe images used for the results in Table 7 were taken from session 2.

The difference amount of average recognition rate of the left light on case is larger than the increasing amount of average recognition rate of the both lights on case by 1.4% approximately because the left light on case is affected by the varying lighting case and variations of the face images caused by different session (session 2), whereas both lights on case is effected by the variations of the face images caused by different session without significant effecting of the varying lighting case since the results shown in Tables 6 and 7 computed through sharing the same lighting conditions.

5.2.5 Recognition Rates of Faces with Varying Synthetic Occlusion Sizes

To evaluate the effectiveness of the proposed approach against the sensitivity to varying synthetic occlusion sizes using the modified AR dataset, experiments have been performed. The face images occluded by a square of $s \times s$ pixels at a random location, as shown in Figure 6 (m)-(p), are used as probe images, while the reference image remained without occlusion, as shown in Figure 6 (a).

The size of the occlusion blocks has been changed from 30×30 , 50×50 , 70×70 , and 100×100 . The average recognition rates of the proposed approach and the other comparative approaches are shown using variant occlusion sizes as shown in Figure 12.

It can be noted from Figure 12 that the average recognition rate of the proposed approach remains almost the same against all occlusion block sizes because this approach can adapt a small part of optimal landmarks to effectively perform the recognition process since each optimal landmark is handled independently from other landmarks.

The performance of the proposed approach significantly outperforms the EBGM and HSO-EBGM approaches, because the landmarks are automatically located in terms of best similarity, and each located optimal landmark is handled independently from other optimal landmarks where each one is based on neighbouring landmarks to compute the similarity. Therefore, the landmarks located in synthetic occlusions will be discarded in recognition process.

The average recognition rate of EBGM and HSO-EBGM approaches is degraded because they are mainly based on the classical EBGM technique in computing the recognition rate where the average similarity of all landmarks is calculated. With a block size of 100×100 , the proposed approach yielded an average recognition rate of 98.5% compared to HSO-EBGM where their average recognition rates dropped significantly around 51.3% because the large part of landmarks of face image located in synthetic occlusions is computed in average recognition rates.

In other words, the proposed approach are about 2 times better than HSO-EBGM in recognizing synthetically occluded faces. These results show the robustness of the proposed approach in handling partial occlusions.

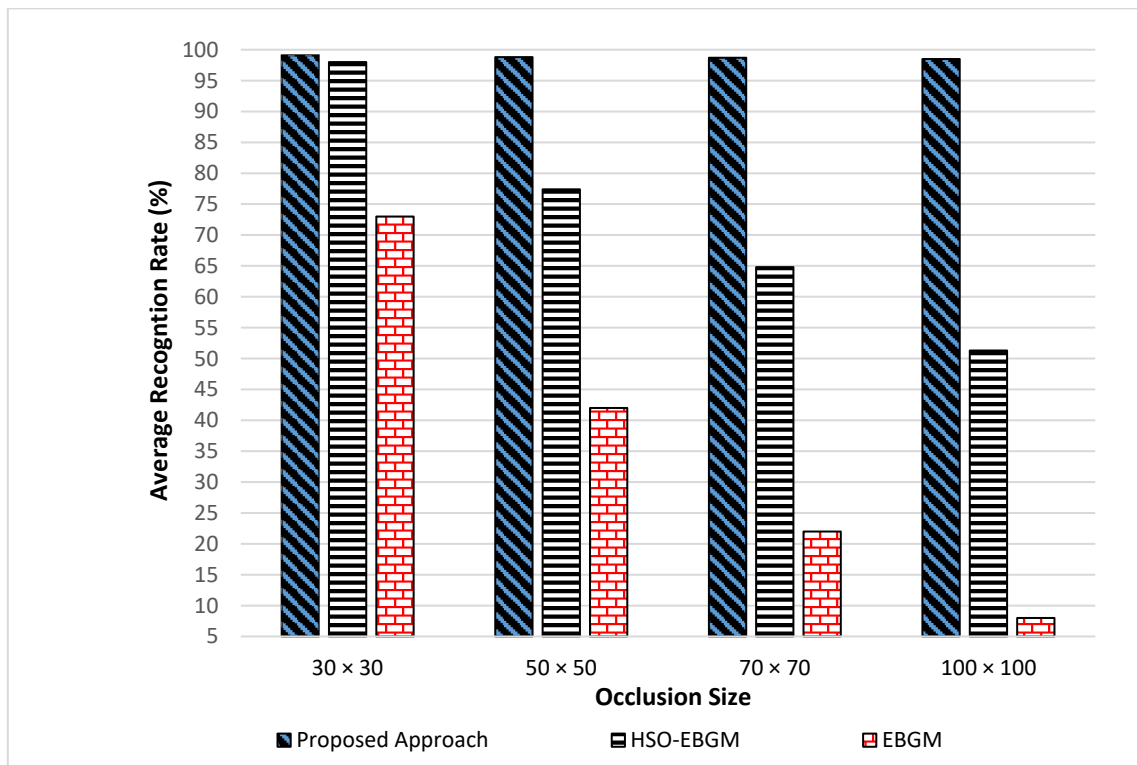


Fig. 12. Average recognition rate observed with varying occlusion sizes by handling the synthetic occlusions as another part of the face

6. Conclusions

In this paper, a new approach was proposed for automatically selecting face landmarks by integrating the classical EBGM face recognition technique with a greedy algorithm where each landmark point (x, y) has a corresponding landmark point either located in the same location in another image or around that location. The locating process of each landmark point is based on neighbouring pixels. A single neutral image was picked as the reference image and set of images similar for probe images which will be matched with that reference image were utilized as the model image. For the recognition process, the similarity between two face images is calculated by averaging the similarity between optimal landmarks and the corresponding landmarks. The performance of the proposed approach was compared against the performance of several approaches using the AR database and the "modified AR" database which we did create it by modifying the AR database by adding synthetic occlusion blocks of different sizes. For evaluation purposes, controlled/ideal conditions, real occlusions, facial expressions, and varying lighting conditions of the AR database, and varying synthetic occlusion sizes of modified AR database are used. Furthermore, the outcomes of the proposed approach were compared with those produced by eight well-established approaches using the same databases. These approaches are LEM, EBGM, AWPPZMA, AWSGA, PISMA, ESM, HSO-EBGM, Gabor-HDLBP+MIBBA. Interestingly, the proposed recognition approach can excel in these other comparative approaches for all tested challenges and variations. Moreover, the proposed approach achieved an average recognition rate comparable to Gabor-HDLBP + MIBBA using controlled/ideal conditions of AR database as well as it outperformed HSO-EBGM and EBGM

approaches by 3% and 13% respectively. Also, the proposed approach outperformed other approaches against real occlusions (faces occluded with scarf and sunglasses), where the proposed approach achieved a better average recognition rate than the EBGM, AWSGA, and PISMA approaches by 54%, 37%, and 25%, respectively. Regarding the varying facial expressions, the performance of the proposed approach stands next to the Gabor-HDLBP + MIBBA approach. Experimental results on recognizing face images using the illumination challenges justify the fact that the proposed approach performed an average recognition rate comparable to the Gabor-HDLBP + MIBBA approach.

When the proposed approach are tested using the synthetic occlusion blocks (face images occluded with random synthetic occlusions of different sizes) of the modified AR database where the synthetic occlusions are automatically discarded by our approach, the performance of proposed approach outperforms the EBGM and HSO-EBGM approaches, where the recognition rate of the proposed approach remain more or less the same as using all occlusion block sizes, whereas the recognition rate of the other benchmark approaches are degraded with increasing the occlusion sizes since these approaches compute the average similarity of all optimal landmarks which are located in the occlusion and face regions of the image. Using a block size of 100×100 , the proposed approach yielded recognition rates of 98.5%, compared to the HSO-EBGM approach, where their recognition rates dropped significantly around 51.3%. In other words, the proposed approach is about 2 times better than the HSO-EBGM approach in recognizing synthetically occluded faces.

Acknowledgement

This research was not funded by any grant.

References

- [1] Payal, Parekh, and Mahesh M. Goyani. "A comprehensive study on face recognition: methods and challenges." *The Imaging Science Journal* 68, no. 2 (2020): 114-127. <https://doi.org/10.1080/13682199.2020.1738741>
- [2] Wu, Hao, Yu Cao, Haiping Wei, and Zhuang Tian. "Face recognition based on Haar like and Euclidean distance." In *Journal of Physics: Conference Series*, vol. 1813, no. 1, p. 012036. IOP Publishing, 2021. <https://doi.org/10.1088/1742-6596/1813/1/012036>
- [3] Paul, Sushil Kumar, Saida Bouakaz, Chowdhury Mofizur Rahman, and Mohammad Shorif Uddin. "Component-based face recognition using statistical pattern matching analysis." *Pattern Analysis and Applications* 24 (2021): 299-319. <https://doi.org/10.1007/s10044-020-00895-4>
- [4] Koc, Mehmet. "A novel partition selection method for modular face recognition approaches on occlusion problem." *Machine Vision and Applications* 32, no. 1 (2021): 35. <https://doi.org/10.1007/s00138-020-01156-4>
- [5] Lahasan, Badr Mohammed, Ibrahim Venkat, Mohammed Azmi Al-Betar, Syaheerah Lebai Lutfi, and Philippe De Wilde. "Recognizing faces prone to occlusions and common variations using optimal face subgraphs." *Applied Mathematics and Computation* 283 (2016): 316-332. <https://doi.org/10.1016/j.amc.2016.02.047>
- [6] Ekenel, Hazım Kemal, and Rainer Stiefelhagen. "Why is facial occlusion a challenging problem?." In *Advances in Biometrics: Third International Conference, ICB 2009, Alghero, Italy, June 2-5, 2009. Proceedings 3*, pp. 299-308. Springer Berlin Heidelberg, 2009. https://doi.org/10.1007/978-3-642-01793-3_31
- [7] Ensari, Tolga, Jan Chorowski, and Jacek M. Zurada. "Occluded face recognition using correntropy-based nonnegative matrix factorization." In *2012 11th International Conference on Machine Learning and Applications*, vol. 1, pp. 606-609. IEEE, 2012. <https://doi.org/10.1109/ICMLA.2012.112>
- [8] Venkat, Ibrahim, Ahamad Tajudin Khader, K. G. Subramanian, and Philippe De Wilde. "Recognizing occluded faces by exploiting psychophysically inspired similarity maps." *Pattern Recognition Letters* 34, no. 8 (2013): 903-911. <https://doi.org/10.1016/j.patrec.2012.05.003>
- [9] Alslibi, Bisan, Ibrahim Venkat, and Mohammed Azmi Al-Betar. "A membrane-inspired bat algorithm to recognize faces in unconstrained scenarios." *Engineering Applications of Artificial Intelligence* 64 (2017): 242-260. <https://doi.org/10.1016/j.engappai.2017.06.018>
- [10] Karamizadeh, Sasan, Shahidan M. Abdullah, and Mazdak Zamani. "An overview of holistic face recognition." *IJRCCCT* 2, no. 9 (2013): 738-741.
- [11] Pankaj, Dhanya S., and M. Wilscy. "Comparison of PCA, LDA and gabor features for face recognition using fuzzy neural network." In *Advances in Computing and Information Technology: Proceedings of the Second International*

- Conference on Advances in Computing and Information Technology (ACITY) July 13-15, 2012, Chennai, India-Volume 2, pp. 413-422. Springer Berlin Heidelberg, 2013. https://doi.org/10.1007/978-3-642-31552-7_43
- [12] Zhao, Wenyi, Arvinth Krishnaswamy, Rama Chellappa, Daniel L. Swets, and John Weng. "Discriminant analysis of principal components for face recognition." *Face recognition: From theory to applications* (1998): 73-85. https://doi.org/10.1007/978-3-642-72201-1_4
- [13] Bartlett, Marian Stewart, Javier R. Movellan, and Terrence J. Sejnowski. "Face recognition by independent component analysis." *IEEE Transactions on neural networks* 13, no. 6 (2002): 1450-1464. <https://doi.org/10.1109/TNN.2002.804287>
- [14] Heisele, Bernd, Purdy Ho, Jane Wu, and Tomaso Poggio. "Face recognition: component-based versus global approaches." *Computer vision and image understanding* 91, no. 1-2 (2003): 6-21. [https://doi.org/10.1016/S1077-3142\(03\)00073-0](https://doi.org/10.1016/S1077-3142(03)00073-0)
- [15] Heisele, Bernd, Thomas Serre, and Tomaso Poggio. "A component-based framework for face detection and identification." *International Journal of Computer Vision* 74 (2007): 167-181. <https://doi.org/10.1007/s11263-006-0006-z>
- [16] Kanan, Hamidreza Rashidy, and Karim Faez. "Recognizing faces using Adaptively Weighted Sub-Gabor Array from a single sample image per enrolled subject." *Image and Vision Computing* 28, no. 3 (2010): 438-448. <https://doi.org/10.1016/j.imavis.2009.06.013>
- [17] Angadi, Shanmukhappa A., and Sanjeevakumar M. Hatture. "Face recognition through symbolic modeling of face graphs and texture." *International Journal of Pattern Recognition and Artificial Intelligence* 33, no. 12 (2019): 1956008. <https://doi.org/10.1142/S0218001419560081>
- [18] Adjabi, Insaf, Abdeldjalil Ouahabi, Amir Benzaoui, and Abdelmalik Taleb-Ahmed. "Past, present, and future of face recognition: A review." *Electronics* 9, no. 8 (2020): 1188. <https://doi.org/10.3390/electronics9081188>
- [19] Phillips, P. Jonathon, Hyeonjoon Moon, Syed A. Rizvi, and Patrick J. Rauss. "The FERET evaluation methodology for face-recognition algorithms." *IEEE Transactions on pattern analysis and machine intelligence* 22, no. 10 (2000): 1090-1104. <https://doi.org/10.1109/34.879790>
- [20] Bolme, David S. "Elastic bunch graph matching." PhD diss., Colorado State University, 2003.
- [21] Senaratne, Rajinda, Saman Halgamuge, and Arthur Hsu. "Face recognition by extending elastic bunch graph matching with particle swarm optimization." *Journal of Multimedia* 4, no. 4 (2009). <https://doi.org/10.4304/jmm.4.4.204-214>
- [22] Wiskott, L., J-M. Fellous, N. Kuiger, and C. von der Malsburg. "Face recognition by elastic bunch graph matching." *IEEE Transactions on Pattern Analysis & Machine Intelligence* 19, no. 07 (1997): 775-779. <https://doi.org/10.1109/34.598235>
- [23] Doumi, A., B., Mahafzah, B. A. & Hiary, H. "Solving traveling salesman problem using genetic algorithm based on efficient mutation operator." *Journal of Theoretical and Applied Information Technology*, 99(15), (2021): 3768–3781.
- [24] Chauhan, Chetan, Ravindra Gupta, and Kshitij Pathak. "Survey of methods of solving tsp along with its implementation using dynamic programming approach." *International journal of computer applications* 52, no. 4 (2012). <https://doi.org/10.5120/8189-1550>
- [25] Pan, Guo, Kenli Li, Aijia Ouyang, and Keqin Li. "Hybrid immune algorithm based on greedy algorithm and delete-cross operator for solving TSP." *Soft Computing* 20 (2016): 555-566. <https://doi.org/10.1007/s00500-014-1522-3>
- [26] Al-Khatib, Ra'ed M., Mohammed Azmi Al-Betar, Mohammed A. Awadallah, Khalid MO Nahar, Mohammed M. Abu Shquier, Ahmad M. Manasrah, and Ahmad Bany Doumi. "MGA-TSP: modernised genetic algorithm for the travelling salesman problem." *International Journal of Reasoning-based Intelligent Systems* 11, no. 3 (2019): 215-226. <https://doi.org/10.1504/IJRIS.2019.102541>
- [27] Asassfeh, Mahmoud, Wesam Almobaideen, And Nadim Obeid. "Spatial Cloaking for Location Privacy Protection of Smart Health Care Systems in Fog Computing." *Journal of Theoretical and Applied Information Technology* 100, no. 14 (2022).
- [28] Glover, Fred W., and Gary A. Kochenberger, eds. *Handbook of metaheuristics*. Vol. 57. Springer Science & Business Media, 2006.
- [29] Martinez, A., and R. Benavente. "The AR face database, CVC." *Copyright of Informatica* (03505596) (1998).
- [30] Mukhiddinov, Mukhriddin, Oybek Djuraev, Farkhod Akhmedov, Abidinabi Mukhamadiyev, and Jinsoo Cho. "Masked face emotion recognition based on facial landmarks and deep learning approaches for visually impaired people." *Sensors* 23, no. 3 (2023): 1080. <https://doi.org/10.3390/s23031080>
- [31] Abdulrahman, Muzammil, Tajuddeen R. Gwadabe, Fahad J. Abdu, and Alaa Eleyan. "Gabor wavelet transform based facial expression recognition using PCA and LBP." In *2014 22nd signal processing and communications applications conference (SIU)*, pp. 2265-2268. IEEE, 2014. <https://doi.org/10.1109/SIU.2014.6830717>

- [32] Yan, H., P. Wang, W. D. Chen, and J. Liu. "Face recognition based on gabor wavelet transform and modular 2dpc." In *2015 International Conference on Power Electronics and Energy Engineering*, pp. 245-248. Atlantis Press, 2015. <https://doi.org/10.2991/peee-15.2015.67>
- [33] Thakral, Shaveta, and Pratima Manhas. "Image processing by using different types of discrete wavelet transform." In *Advanced Informatics for Computing Research: Second International Conference, ICAICR 2018, Shimla, India, July 14–15, 2018, Revised Selected Papers, Part I 2*, pp. 499-507. Springer Singapore, 2019. https://doi.org/10.1007/978-981-13-3140-4_45
- [34] Hegele, Marius, Philipp Metzler, Sebastian Beichter, Friedrich Wiegel, and Veit Hagenmeyer. "An Efficient Greedy Algorithm for Real-World Large-Scale Electric Vehicle Charging." In *Proceedings of the 14th ACM International Conference on Future Energy Systems*, pp. 415-426. 2023. <https://doi.org/10.1145/3575813.3597349>
- [35] Lim, Ching Lih. "A Suite of Greedy Methods for Set Cover Computation." PhD diss., University of Melbourne, Department of Computing and Information Systems, 2015.
- [36] Gao, Yongsheng, and Maylor KH Leung. "Face recognition using line edge map." *IEEE transactions on pattern analysis and machine intelligence* 24, no. 6 (2002): 764-779. <https://doi.org/10.1109/TPAMI.2002.1008383>
- [37] Belhumeur, Peter N., Joao P. Hespanha, and David J. Kriegman. "Eigenfaces vs. fisherfaces: Recognition using class specific linear projection." *IEEE Transactions on pattern analysis and machine intelligence* 19, no. 7 (1997): 711-720. <https://doi.org/10.1109/34.598228>
- [38] Kanan, Hamidreza Rashidy, Karim Faez, and Yongsheng Gao. "Face recognition using adaptively weighted patch PZM array from a single exemplar image per person." *Pattern Recognition* 41, no. 12 (2008): 3799-3812. <https://doi.org/10.1016/j.patcog.2008.05.024>
- [39] Gottumukkal, Rajkiran, and Vijayan K. Asari. "An improved face recognition technique based on modular PCA approach." *Pattern Recognition Letters* 25, no. 4 (2004): 429-436. <https://doi.org/10.1016/j.patrec.2003.11.005>
- [40] Chen, Weiping, and Yongsheng Gao. "Face recognition using ensemble string matching." *IEEE Transactions on Image Processing* 22, no. 12 (2013): 4798-4808. <https://doi.org/10.1109/TIP.2013.2277920>
- [41] Wright, John, Allen Y. Yang, Arvind Ganesh, S. Shankar Sastry, and Yi Ma. "Robust face recognition via sparse representation." *IEEE transactions on pattern analysis and machine intelligence* 31, no. 2 (2008): 210-227. <https://doi.org/10.1109/TPAMI.2008.79>
- [42] Varma, Teena, Swarali Gaonkar, and Vailantina Fernandes. "Face Recognition using Histogram."
- [43] Cheng, Pengfei, and Siche Pan. "Learning from Face recognition under occlusion." In *2022 International Conference on Big Data, Information and Computer Network (BDICN)*, pp. 721-727. IEEE, 2022. <https://doi.org/10.1109/BDICN55575.2022.00140>
- [44] Ma, Xiang, Qinqin Ma, Qian Ma, and Xiao Han. "Robust face recognition for occluded real-world images using constrained probabilistic sparse network." *IET Image Processing* 16, no. 5 (2022): 1359-1375. <https://doi.org/10.1049/ipr2.12414>
- [45] Hemathilaka, Susith, and Achala Aponso. "A comprehensive study on occlusion invariant face recognition under face mask occlusion." *arXiv preprint arXiv:2201.09089* (2022). <https://doi.org/10.5121/csit.2021.111804>
- [46] Moungsouy, Warot, Thanawat Tawanbunjerd, Nutcha Liamsomboon, and Worapan Kusakunniran. "Face recognition under mask-wearing based on residual inception networks." *Applied Computing and Informatics* (2022). <https://doi.org/10.1108/ACI-09-2021-0256>
- [47] Chen, Yuekun, Shuaishi Liu, Dongxu Zhao, and Wenkai Ji. "Occlusion facial expression recognition based on feature fusion residual attention network." *Frontiers in Neurorobotics* 17 (2023). <https://doi.org/10.3389/fnbot.2023.1250706>
- [48] Sinha, Pawan, Benjamin Balas, Yuri Ostrovsky, and Richard Russell. "Face recognition by humans: Nineteen results all computer vision researchers should know about." *Proceedings of the IEEE* 94, no. 11 (2006): 1948-1962. <https://doi.org/10.1109/JPROC.2006.884093>
- [49] Hinson, John M., and J. E. R. Staddon. "Matching, maximizing, and hill-climbing." *Journal of the experimental analysis of behavior* 40, no. 3 (1983): 321-331. <https://doi.org/10.1901/jeab.1983.40-321>
- [50] Al-Khatib, Ra'ed M., Mohammed Azmi Al-Betar, Mohammed A. Awadallah, Khalid MO Nahar, Mohammed M. Abu Shquier, Ahmad M. Manasrah, and Ahmad Bany Doumi. "MGA-TSP: modernised genetic algorithm for the travelling salesman problem." *International Journal of Reasoning-based Intelligent Systems* 11, no. 3 (2019): 215-226. <https://doi.org/10.1504/IJRIS.2019.102541>